Energy-Efficient Joint Congestion Control and Resource Optimization in Heterogeneous Cloud Radio Access Networks

Jian Li, Mugen Peng†, *Senior Member, IEEE*, Yuling Yu, and Zhiguo Ding

Abstract—The heterogeneous cloud radio access network (H-CRAN) is a promising paradigm which integrates the advantages of cloud radio access network (C-RAN) and heterogeneous network (HetNet). In this paper, we study the joint congestion control and resource optimization to explore the energy efficiency (EE)-guaranteed tradeoff between throughput utility and delay performance in a downlink slotted H-CRAN. We formulate the considered problem as a stochastic optimization problem, which maximizes the utility of average throughput and maintains the network stability subject to required EE constraint and transmit power consumption constraints by traffic admission control, user association, resource block allocation and power allocation. Leveraging on the Lyapunov optimization technique, the stochastic optimization problem can be transformed and decomposed into three separate subproblems which can be solved concurrently at each slot. The third mixed-integer nonconvex subproblem is efficiently solved utilizing the continuity relaxation of binary variables and the Lagrange dual decomposition method. Theoretical analysis shows that the proposal can quantitatively control the throughput-delay performance tradeoff with required EE performance. Simulation results consolidate the theoretical analysis and demonstrate the advantages of the proposal from the prospective of queue stability and power consumption.

Index Terms—Heterogeneous cloud radio access networks (H-CRANs), energy efficiency (EE), congestion control, resource optimization, Lyapunov optimization.

I. INTRODUCTION

Recently, the mobile operators are facing the continuously growing demand for ubiquitous high-speed wireless access and the explosive proliferation of smart phones. Justified by the urgent trend and projecting the demand a decade ahead, a so-called 100 times spectral efficiency (SE) boost and 1000 times energy efficiency (EE) improvement compared to the current fourth generation (4G) wireless systems are required [1]. The increasingly demands make it more challenging for operators to manage and operate wireless networks and provide required quality of service (QoS) efficiently. Therefore, the fifth generation (5G) wireless networks are expected to fulfill these goals by putting forward new wireless network architectures, advanced signal processing, and networking technologies [2], [3].

Jian Li (e-mail: lijian.wspn@gmail.com), Mugen Peng (corresponding author, e-mail: pmg@bupt.edu.cn), Yuling Yu (e-mail: aliceyul215@gmail.com) are with the Key Laboratory of Universal Wireless Communications for Ministry of Education, Beijing University of Posts and Telecommunications, China. Zhiguo Ding (e-mail: z.ding@lancaster.ac.uk) is with the School of Computing and Communications, Lancaster University, LA1 4WA, UK.

By leveraging cloud computing technologies, the cloud radio access network (C-RAN) has emerged as a promising solution for providing good performance in terms of both SE and EE across software defined wireless communication networks [4]. In C-RANs, the remote radio heads (RRHs) configured only with some front radio frequency (RF) functionalities are connected to the baseband unit (BBU) pool through fronthaul links (e.g., optical fibers) to enable cloud computing-based large-scale cooperative signal processing. However, the constrained fronthaul link between the RRH and the BBU pool presents a performance bottleneck to large-scale cooperation gains. Furthermore, real-time voice service and control signalling are not efficiently supported in C-RANs. Therefore, the traditional C-RAN must be enhanced and even evolved.

Motivated by solving the aforementioned challenges, the heterogeneous cloud radio access network (H-CRAN) has been proposed to combine the advantages of both C-RANs and heterogeneous networks (HetNets) in our prior works [5] [6]. As shown in Fig. 1, the high power nodes (HPNs) are configured with the entire communication functionalities from physical to network layers, and the delivery of control and broadcast signalling is shifted from RRHs to HPNs, which alleviates the capacity and time delay constraints on the fronthaul. The BBU pool is interfaced to the HPN for the inter-tier interference coordination. H-CRANs decouple the control and user planes, and support the adaptive signaling/control mechanism between connection-oriented and connectionless modes, which can achieve significant overhead savings in the radio connection/release. For a time-varying H-CRAN that adopts orthogonal frequency division multiple access (OFDMA), besides of power and resource block (RB) allocation, the traffic admission, the user association are also critical for improving key performances.

A. Related Works

The resource optimization is significantly important to highlight the great potentials of H-CRANs. The EE performance metric has become a new design goal due to the sharp increase of the carbon emission and operating cost of wireless communication systems [7]. The tradeoff relationship between EE and SE has attracted growing interests in the design of energy-efficient radio resource optimization algorithms for wireless communication systems [8] [9]. Power allocation was studied in [10] to address the EE-SE tradeoff in the downlink
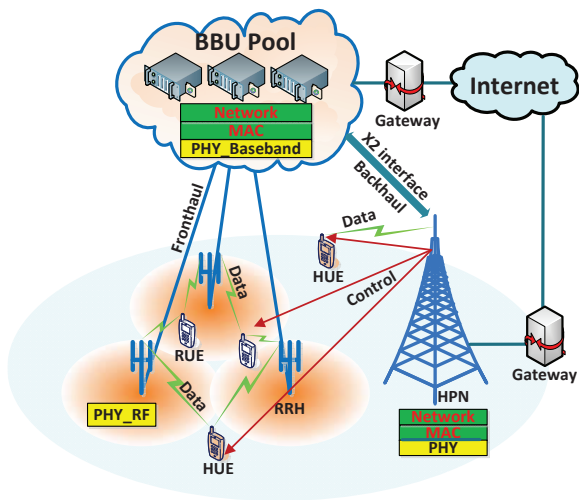
Fig. 1.   The heterogeneous cloud radio access networks (H-CRANs)

multi-user distributed antenna system (DAS) with proportional rate constraints. The authors of [11]–[13] jointly consider multi-dimensional resource optimization, such as beamforming optimization, power allocation, and RB assignment, to explore the EE-SE tradeoff in OFDMA networks. The EE-SE tradeoff also got deep investigation in Device-to-Device (D2D) communications and relay-aided cellular networks [14]–[16].

However, the aforementioned literatures are typically based on the full buffer assumptions and snapshot-based models. This indicates that the stochastic and time-varying features of traffic arrivals are not considered into the formulations. Therefore, only the physical layer performance metrics such as SE and EE are optimized and the resulting control policy is only adaptive to channel state information (CSI). In practice, delay is also a key metric to measure the QoS, which is also neglected in these literatures.

Contrary to the static models used in the EE-SE tradeoff, the power-delay tradeoff is usually investigated from the long-term average perspective in a time-varying system. The authors of [17] and [18] aimed to dynamically optimize the power and subband allocations to achieve the Pareto optimal tradeoff between power consumption and average delay in OFDMA systems. In [19], a theoretical framework was presented to analyze power-delay tradeoff in a time-varying OFDMA system with imperfect CSIT. Adaptive antenna selection and power allocation were exploited in [20] to compromise the power consumption and average delay in downlink distributed antenna systems. By devising delay-aware beamforming algorithm, [21] studied the power-delay tradeoff in multi-user MIMO systems.

As a common feature, [17]–[21] assumed that the random traffic arrival rate is inside the network capacity region. This indicates that admission control is unnecessary. Moreover, throughput was not formulated into the problem, thus the results for power-delay tradeoff can hardly give insights into energy-efficient resource optimization problems.

B. Main Contributions

In this paper, considering the traffic admission control, the throughput, as in [22] and [23], is defined as the maximum amount of admissible traffic that H-CRANs can stably carry, and therefore it to some extent reflects SE. Based on this, we try to incorporate throughput, delay, and EE into a theoretical framework, and effectively balance throughput and delay when certain EE requirement is guaranteed for any traffic arrival rate in slotted H-CRANs. The major contributions of this paper are twofold.

- The congestion control is incorporated into the radio resource optimization model for slotted H-CRANs without prior-knowledge of random traffic arrival rates and channel statistics. The decomposed subproblems can be solved concurrently at each slot with the online observation of traffic queues and virtual queues, which have been determined by the joint optimization results at the previous slot. Simulations demonstrate the advantages of the proposal from the prospective of queue stability and power savings.
- Using the framework of Lyapunov optimization, we put forward a formulation to quantitatively strike a balance between average throughput and average delay, meanwhile guarantee the required EE performance of H-CRANs. Only by adjusting a control parameter, the proposal provides a controllable method to balance the throughput-delay performance on demand, which in turn adaptively affects admission control and resource allocation.

The rest of this paper is organized as follows. Section II will describe the system model and formulate the stochastic optimization problem. Based on the framework of Lyapunov optimization, the stochastic optimization problems of traffic admission control, user association, RB and power allocation will be transformed and decomposed in Section III. The challenging subproblem for user association, RB and power allocation will be solved in Section IV. The performance bounds of proposal will be analyzed in section V. Numerical simulations will be shown in Section VI. Finally, Section VII will summarize this paper.

II. SYSTEM MODEL AND PROBLEM FORMULATION

In this section, we begin with describing the physical layer model, followed by introducing the queue dynamics and the queue stability. We then formally formulate the stochastic optimization problem. For convenience, the notations used are listed in Table I.

A. Physical Layer Model

The downlink transmission in an OFDMA-based H-CRAN is considered, in which one HPN and N RRHs are consisted. Since the HPN is mainly used to deliver the control signalling and guarantee the basic coverage for certain area, the UEs with low traffic arrival rates are more likely served by HPN and they are labeled as HUEs. Meanwhile, since the RRHs are efficient to provide high bit rates, the user equipments (UEs)

TABLE I
SUMMARY OF NOTATIONS

Notation	Description
$\mathcal{R}$	Set of RRHs
$\mathcal{U}_H$	Set of HUEs
$\mathcal{U}_R$	Set of RUEs
$\mathcal{K}_H$	Set of RBs used by RRHs
$\mathcal{K}_R$	Set of RBs used by the HPN
$s_m(t)$	Association indicator for the HUE m at the time slot t
$g_{ijk}(t)$	CSI on the RB k from the RRH i to the RUE j at the slot t
$g_{imk}(t)$	CSI on the RB k from the RRH i to the HUE m at the slot t
$g_{ml}(t)$	CSI on the RB l from the HPN to the HUE m at the slot t
$c_l^H(t)$	RB usage indicator for the RB l of the HPN at the slot t
$c_k^R(t)$	RB usage indicator for the RB k of RRHs at the slot t
$p_{ijk}(t)$	Allocated power for the RUE j occupying the RB k of the RRH i at the slot t
$p_{imk}(t)$	Allocated power for the HUE m occupying the RB k of the RRH i at the slot t
$p_{ml}(t)$	Allocated power for the HUE m occupying the RB l of the HPN at the slot t
$a_{jk}(t)$	Allocation of the RB k of RRHs to the RUE j at the slot t
$a_{mk}(t)$	Allocation of the RB k of RRHs to the HUE m at the slot t
$b_{ml}(t)$	Allocation of the RB l of the HPN to the HUE m at the slot t
$\mu_m(t)$	Transmit rate of the HUE m at the slot t
$\mu_j(t)$	Transmit rate of the RUE j at the slot t
$R_m(t)$	The amount of admitted traffics for the HUE m at the slot t
$R_j(t)$	The amount of admitted traffics for the RUE j at the slot t
$Q_m(t)$	Traffic buffering queue length for the HUE m at the slot t
$Q_j(t)$	Traffic buffering queue length for the RUE j at the slot t
$\gamma_m(t)$	Auxiliary variable for the throughput of the HUE m at the slot t
$\gamma_j(t)$	Auxiliary variable for the throughput of the RUE j at the slot t
$H_m(t)$	Virtual queue length for the HUE m with arrival γ_m at the slot t
$H_j(t)$	Virtual queue length for the RUE j with arrival γ_j at the slot t
$Z(t)$	Virtual queue length for the average EE constraint at the slot t
x_{mk}	Continuous auxiliary variable for RB allocation a_{mk}
y_{ml}	Continuous auxiliary variable for RB allocation b_{ml}
w_{ijk}	Auxiliary variable for power allocation p_{ijk}
v_{imk}	Auxiliary variable for power allocation p_{imk}
u_{ml}	Auxiliary variable for power allocation p_{ml}

with high traffic arrival rates will be served by the RRHs. Let $\mathcal{R} = \{1, 2, ..., N\}$ denote the set of RRHs, let $\mathcal{U}_H$ denote the set of HUEs and let $\mathcal{U}_R$ denote the set of RUEs. To completely avoid the severe inter-tier interferences, the RBs of H-CRAN are partitioned and assigned respectively to the RRH and the HPN tiers. Let $\mathcal{K}_R$ and $\mathcal{K}_H$ denote the set of RBs used by RRH tier and HPN tier, respectively. Let W and W_0 denote the system bandwidth and the bandwidth of each RB, respectively. Any UE that is associated with RRH tier receives signal simultaneously from multiple cooperative RRHs on allocated RBs, and the RBs allocated to different UEs are orthogonal, it is thus inter-RRH interference-free among UEs. The network is assumed to operate in slotted time with slot duration τ and indexed by t.

The HUEs can be associated with RRH tier to get more transmission opportunity when the traffic load of HPN becomes heavier, while the RUEs are served only by RRHs, which is usually in accordance with the practice. The user association strategy plays an important role in improving the utilization efficiencies of limited radio resources in an H-CRAN. Let the binary variable $s_m(t)$ indicate the user association of the HUE m at the slot t, which is 1 when the HUE m is associated with the RRH tier or 0 when it is associated with the HPN. Let $g_{ijk}(t)$, $g_{imk}(t)$ and $g_{ml}(t)$ represent the CSIs on the RB k from the RRH i to the RUE j, the RB k from the RRH i to the HUE m, the RB l from the HPN to the HUE m, respectively. Note that these CSIs account for the antenna gain, beamforming gain, path loss, shadow fading, fast fading, and noise together. In this paper, as the RB allocation for both RRHs and HPN tiers in OFDMA-based H-CRANs are focused, the antenna configuration and beamforming design are not specified, and neither of them affects the general formulation. The CSIs are assumed to be independently and identically distributed (i.i.d.) over slots, and takes values in a finite state place. Let $p_{ijk}(t)$ denote the allocated transmit power for RUE j on RB k from RRH i at slot t, let $p_{imk}(t)$ denote the allocated transmit power for HUE m on RB k from RRH i if HUE m is associated with RRH tier at slot t, and let $p_{ml}(t)$ denote the allocated transmit power for HUE m on RB l from HPN if HUE m is associated with HPN at slot t. Furthermore, let the binary variable $a_{jk}(t)$ and $a_{mk}(t)$ indicate the allocation of RB k of RRH tier to RUE j and HUE m at slot t, respectively, and let $b_{ml}(t)$ indicate the allocation of RB l of HPN to HUE m at slot t, then we have the following non-reuse constraints

$$c_k^R(t) = \sum_{j \in \mathcal{U}_R} a_{jk}(t) + \sum_{m \in \mathcal{U}_H} s_m(t) a_{mk}(t) \leq 1, \quad (1)$$

$$c_l^H(t) = \sum_{m \in \mathcal{U}_H} (1 - s_m(t)) b_{ml}(t) \leq 1. \quad (2)$$

for the RRH tier and HPN tier, respectively.

For the UEs that are served by RRHs (including all the RUEs and some associated HUEs), the maximum ratio combining (MRC) is assumed to be adopted. Therefore, the transmit rate of RUE j and HUE m at slot t is given by

$$\mu_j(t) = \sum_{k \in \mathcal{K}_R} a_{jk}(t) W_0 \log_2(1 + \sum_{i \in \mathcal{R}} p_{ijk}(t) g_{ijk}(t)), \quad (3)$$

$$\mu_m(t) = (1 - s_m(t)) \sum_{l \in \mathcal{K}_H} b_{ml}(t) W_0 \log_2(1 + g_{ml}(t) p_{ml}(t)) + s_m(t) \sum_{k \in \mathcal{K}_R} a_{mk}(t) W_0 \log_2(1 + \sum_{i \in \mathcal{R}} p_{imk}(t) g_{imk}(t)), \quad (4)$$

respectively. Accordingly, the total transmit rate of the network is given by

$$\mu_{\text{sum}}(t) = \sum_{m \in \mathcal{U}_H} \mu_m(t) + \sum_{j \in \mathcal{U}_R} \mu_j(t), \quad (5)$$

With the resource allocations, the transmit power of RRH i and HPN is given by

$$p_i(t) = \sum_{j \in \mathcal{U}_R} \sum_{k \in \mathcal{K}_R} a_{jk}(t) p_{ijk}(t) + \sum_{m \in \mathcal{U}_H} \sum_{k \in \mathcal{K}_R} s_m(t) a_{mk}(t) p_{imk}(t), \quad (6)$$

$$p_H(t) = \sum_{m \in \mathcal{U}_H} \sum_{l \in \mathcal{K}_H} (1 - s_m(t)) b_{ml}(t) p_{ml}(t), \quad (7)$$

respectively. Accordingly, the total power consumption of the network is given by

$$p_{\text{sum}}(t) = \sum_{i \in \mathcal{R}} \varphi_{\text{eff}}^R p_i(t) + p_{\text{c}}^R + \varphi_{\text{eff}}^H p_H(t) + p_{\text{c}}^H, \quad (8)$$

where φ_{eff}^R and φ_{eff}^H are the drain efficiency of RRH and HPN, respectively, p_{c}^R and p_{c}^H are the static power consumption of RRHs and HPN, respectively, including the circuit power, the fronthaul power consumption and the backhaul power consumption.

B. Queue Dynamics and Queue Stability

In the considered H-CRAN, separate buffering queues are maintained for each UE. Let $Q_m(t)$ and $Q_j(t)$ denote the length of buffering queues maintained for HUE m and RUE j, respectively. Let $A_m(t)$ and $A_j(t)$ denote the amount of random traffic arrivals at slot t destined for HUE $m \in \mathcal{U}_H$ and RUE $j \in \mathcal{U}_R$, respectively.

Assumption 1 (Random Traffic Arrivals Model): Assume that $A_m(t)$ and $A_j(t)$ are i.i.d. over time slots according to a general distribution, which are independent w.r.t. m and j. Furthermore, there exists certain peak amount of traffic arrivals $A_m^{\max}$ and $A_j^{\max}$, respectively, which satisfying $A_m(t) \leq A_m^{\max}$ and $A_j(t) \leq A_j^{\max}$.

In practice, the statistics of $A_m(t)$ and $A_j(t)$ are usually unknown to H-CRANs, and the achievable capacity region is usually difficult to estimate, the situation that the exogenous arrival rates are outside of the network capacity region may occur. In this situation, the traffic queues cannot be stabilized without a transport layer flow control mechanism to limit the amount of data that is admitted. To this end, the H-CRAN tries to maximize its utility by admitting as many traffic datas as possible, and to minimize the penalty from traffic congestion by transmitting as many traffic datas as possible with the limited radio resources. Let $R_m(t)$ and $R_j(t)$ denote the amount of admitted traffic datas out of the potentially substantial traffic arrivals for HUE m and RUE j, respectively. Therefore, the traffic buffering queues for HUE m and RUE j evolve as

$$Q_m(t+1) = \max\{Q_m(t) - \mu_m(t)\tau, 0\} + R_m(t), \quad (9)$$

$$Q_j(t+1) = \max\{Q_j(t) - \mu_j(t)\tau, 0\} + R_j(t), \quad (10)$$

respectively, where we have $0 \leq R_m(t) \leq A_m(t)$ and $0 \leq R_j(t) \leq A_j(t)$ at each slot.

To model the impacts of joint congestion control and resource allocation on the average delay and the achieved throughput utility, the definition of network stability will be formally given.

Definition 1: A single discrete time queue $Q(t)$ is strongly stable if

$$\limsup_{T \to \infty} \frac{1}{T} \sum_{t=0}^{T-1} \mathbb{E}[Q(t)] < \infty \quad (11)$$

Definition 2: A network of queues is strongly stable if all the individual queues of the network are strongly stable.

To guarantee certain EE requirement when dynamically making congestion control and resource optimization for the H-CRAN. As in [24], the definition of EE is given as follows.

Definition 3: The EE of considered H-CRAN is defined as the ratio of the long-term time averaged total transmit rate to the corresponding long-term time averaged total power consumption in the unit of bits/Hz/J, which is given by

$$\eta_{EE} = \frac{\lim\limits_{T \to \infty} \frac{1}{T} \sum\limits_{t=0}^{T-1} \mathbb{E}[\mu_{sum}(t)]}{W \lim\limits_{T \to \infty} \frac{1}{T} \sum\limits_{t=0}^{T-1} \mathbb{E}[p_{sum}(t)]} = \frac{\bar{\mu}_{sum}}{W \bar{p}_{sum}}, \quad (12)$$

A queue is strongly stable if it has a bounded time average queue backlog. According to the Little's Theorem [25], the average delay is proportional to the average queue length for a given traffic arrival rate. Furthermore, when a network of traffic queues is strongly stable, the average achieved throughput can be given by the time averaged amount of admitted exogenous traffic arrivals. Therefore, the average throughput for HUE and RUE is expressed as

$$\bar{r}_m = \lim_{T \to \infty} \frac{1}{T} \sum_{t=0}^{T-1} R_m(t), \quad (13)$$

$$\bar{r}_j = \lim_{T \to \infty} \frac{1}{T} \sum_{t=0}^{T-1} R_j(t), \quad (14)$$

respectively.

C. Problem Formulation

The profit brought by dynamic joint congestion control and resource optimization can be characterized by the utility of average throughput, which is given by

$$U(\bar{\mathbf{r}}) = \alpha \sum_{j \in \mathcal{U}_R} g_R(\bar{r}_j) + \beta \sum_{m \in \mathcal{U}_H} g_H(\bar{r}_m), \quad (15)$$

where $\bar{\mathbf{r}} = [\bar{r}_m, \bar{r}_j : m \in \mathcal{U}_H, j \in \mathcal{U}_R]$ is the vector of average throughput for all UEs, $g_R(.)$ and $g_H(.)$ are the non-decreasing concave utility function for RUEs and HUEs, respectively, α and β are the positive utility prices which indicate the relative importance of corresponding utility functions.

Let $\mathbf{r} = [R_j(t), R_m(t) : j \in \mathcal{U}_R, m \in \mathcal{U}_H]$, $\mathbf{s}(t) = [s_m(t) : m \in \mathcal{U}_H]$, $\mathbf{p} = [p_{ijk}(t), p_{imk}(t), p_{ml}(t) : j \in \mathcal{U}_R, m \in \mathcal{U}_H, i \in \mathcal{R}, k \in \mathcal{K}_R, l \in \mathcal{K}_H]$, $\mathbf{a} = [a_{jk}(t), a_{mk}(t), b_{ml}(t) : j \in \mathcal{U}_R, m \in \mathcal{U}_H, k \in \mathcal{K}_R, l \in \mathcal{K}_H]$ denote the vectors of traffic admission, user association, power allocation and RB allocation, respectively. To maximize the throughput utility of networks and ensure the strong stability of traffic queues at the same time by joint congestion control and resource optimization, the stochastic optimization problem can be formulated as

follows:

$$\max_{\{\mathbf{r},\mathbf{s},\mathbf{p},\mathbf{a}\}} U(\bar{\mathbf{r}})$$
$$\text{s.t.} \quad C1: c_k^R(t) \leq 1, \forall k, t,$$
$$C2: c_l^H(t) \leq 1, \forall l, t,$$
$$C3: p_i(t) \leq p_i^{\max}, \forall i, t,$$
$$C4: p_H(t) \leq p_H^{\max}, \forall t,$$
$$C5: \eta_{EE} \geq \eta_{EE}^{\mathrm{req}},$$
$$C6: Q_m(t) \text{ and } Q_j(t) \text{ are strongly stable}, \forall m, j,$$
$$C7: R_m(t) \leq A_m(t), R_j(t) \leq A_j(t), \forall m, j, t,$$
$$C8: a_{jk}(t), a_{mk}(t), b_{ml}(t), s_m(t) \in \{0,1\}, \forall j, k, m, l, t.$$
$$(16)$$

where $p_i^{\max}$ and $p_H^{\max}$ denote the maximum transmit power consumption of RRH i and HPN, respectively, and η_{EE}^{req} denote the required EE of the network. C1 and C2 ensure that each RB of both tiers cannot be allocated to more than one UE. C3 and C4 restrict the instantaneous transmit power of each RRH and HPN. C5 makes the EE performance above predefined level. C6 ensures the queue stability to guarantee a finite average delay for each queue. C7 ensures that the amount of admitted traffics cannot be more than that of arrivals, C8 is the binary constraint for the RB allocation and the user association.

For realistic H-CRANs, on one hand, the bursty traffic arrivals are time-varying and unpredictable, and the key parameters are hardly captured, which makes it infeasible to obtain optimal solution in an offline manner; on the other hand, the dense deployment of RRHs in H-CRANs exacerbates the computational complexity of centralized solution. Therefore, an online and low-complexity solution to make decisions effectively on user association, RB and power allocation will be designed in the following sections.

III. DYNAMIC OPTIMIZATION UTILIZING LYAPUNOV OPTIMIZATION

In response to the challenges of problem (16), we take advantage of Lyapunov optimization techniques [22] to design an online control framework, which is able to make all three important control decisions concurrently, including traffic admission control, user association, RB and power allocation.

A. Equivalent Formulation via Virtual Queues

The formulated dynamic resource optimization problem in (16) involves maximizing a non-decreasing concave function of average throughputs, which is a bottleneck for solution. To address this issue, the non-negative auxiliary variables $\gamma_m(t)$ and $\gamma_j(t)$ are introduced to transform problem (16) into an equivalent optimization problem with a time averaged utility function of instantaneous throughputs instead of a utility function of average throughputs. Let $\boldsymbol{\gamma} = [\gamma_m(t), \gamma_j(t) : m \in \mathcal{U}_H, j \in \mathcal{U}_R]$ be the vector of introduced auxiliary variables, then we have the following equivalent problem:

$$\max_{\{\mathbf{r},\mathbf{s},\mathbf{p},\mathbf{a},\boldsymbol{\gamma}\}} \lim_{T \to \infty} \frac{1}{T} \sum_{t=0}^{T-1} U(\boldsymbol{\gamma}(t))$$
$$\text{s.t.} \quad C1 - C8,$$
$$C9: \gamma_j(t) \leq A_j^{\max}, \gamma_m(t) \leq A_m^{\max}, \forall j, m, t,$$
$$C10: \bar{\gamma}_j \leq \bar{r}_j, \bar{\gamma}_m \leq \bar{r}_m, \forall j, m.$$
$$(17)$$

where $U(\boldsymbol{\gamma}(t)) = \alpha \sum_{j \in \mathcal{U}_R} g_R(\gamma_j(t)) + \beta \sum_{m \in \mathcal{U}_H} g_H(\gamma_m(t))$, $\bar{\gamma}_j = \lim_{T \to \infty} \frac{1}{T} \sum_{t=0}^{T-1} \gamma_j(t)$ and $\bar{\gamma}_m = \lim_{T \to \infty} \frac{1}{T} \sum_{t=0}^{T-1} \gamma_m(t)$. Let $\mathbf{r}^{\mathrm{opt}}$, $\mathbf{s}^{\mathrm{opt}}$, $\mathbf{p}^{\mathrm{opt}}$ and $\mathbf{a}^{\mathrm{opt}}$ denote the optimal solution to the original problem (16), and let $\mathbf{r}^*$, $\mathbf{s}^*$, $\mathbf{p}^*$, $\mathbf{a}^*$, and $\boldsymbol{\gamma}^*$ denote the optimal solution to the equivalent problem (17), then we have the following theorem.

Theorem 1: *The optimal solution for the transformed problem (17) can be directly turned into an optimal solution for the original problem (16). Specifically, the optimal solution for the original problem can be obtained as* $\mathbf{r}^{\mathrm{opt}} = \mathbf{r}^*$, $\mathbf{s}^{\mathrm{opt}} = \mathbf{s}^*$, $\mathbf{p}^{\mathrm{opt}} = \mathbf{p}^*$, *and* $\mathbf{a}^{\mathrm{opt}} = \mathbf{a}^*$.

Proof: Please refer to Appendix A. □

To ensure the average constraints for auxiliary variables in C10, the virtual queues $H_m(t)$ and $H_j(t)$ are introduced for each HUE and each RUE, respectively, and they evolve as

$$H_m(t+1) = \max\{H_m(t) - R_m(t), 0\} + \gamma_m(t), \quad (18)$$

$$H_j(t+1) = \max\{H_j(t) - R_j(t), 0\} + \gamma_j(t), \quad (19)$$

where $H_m(0) = 0$, $H_j(0) = 0$, $\gamma_m(t)$ and $\gamma_j(t)$ will be optimized at each slot.

Similarly, to ensure the EE performance constraint C5, the virtual queue $Z(t)$ with initial value $Z(0) = 0$ is also introduced, and it evolves as

$$Z(t+1) = \max\{Z(t) - \mu_{\mathrm{sum}}(t), 0\} + W\eta_{EE}^{\mathrm{req}} p_{\mathrm{sum}}(t), \quad (20)$$

Intuitively, the auxiliary variables $\gamma_m(t)$, $\gamma_j(t)$ and $W\eta_{EE}^{\mathrm{req}} p_{\mathrm{sum}}(t)$ can be looked as the arrivals of virtual queues $H_m(t)$, $H_j(t)$ and $Z(t)$, respectively, while $R_m(t)$, $R_j(t)$ and $\mu_{\mathrm{sum}}(t)$ can be looked as the service rate of such virtual queues.

Theorem 2: *The constraints C5 and C10 can be satisfied only when the virtual queues $H_m(t)$, $H_j(t)$ and $Z(t)$ are stable.*

Proof: Please refer to Appendix B. □

B. Problem Transformulation via Lyapunov Optimization

Let $\chi(t) = [Q_m(t), Q_j(t), H_m(t), H_j(t), Z(t) : m \in \mathcal{U}_H, j \in \mathcal{U}_R]$ denote the vector of the traffic queues and virtual queues. To represent a scalar metric of queue congestion, the quadratic Lyapunov function is defined as

$$L(\chi(t)) = \frac{1}{2}\left(\sum_{m \in \mathcal{U}_H} Q_m^2(t) + \sum_{m \in \mathcal{U}_H} H_m^2(t) + \sum_{j \in \mathcal{U}_R} Q_j^2(t) + \sum_{j \in \mathcal{U}_R} H_j^2(t) + Z^2(t)\right),$$
$$(21)$$

where a small value of $L(\chi(t))$ implies that both actual queues and virtual queues are small and the queues have strong stability. Therefore, the queue stability can be ensured by persistently pushing the Lyapunov function towards a lower congestion state. To stabilize the traffic queues, while additionally satisfy some average constraints and optimize the system throughput utility, the Lyapunov conditional drift-minus-utility function is defined as

$$\Delta(\chi(t)) = \mathbb{E}[L(\chi(t+1)) - L(\chi(t)) - VU(\boldsymbol{\gamma}(t))|\chi(t)], \quad (22)$$

where the control parameter $V(V \geq 0)$ represents the emphasis on utility maximization compared to queue stability. By

adjusting V, flexible design choices among various tradeoff points between queue delay and throughput utility can be made by operators. With the dynamics of practical traffic queues and introduced virtual queues, the upper bound of drift-plus-utility is derived in the following lemma.

Lemma 1: At slot t, for any observed queue state, the Lyapunov drift-minus-utility of an H-CRAN with any joint congestion control and resource optimization strategy satisfies the following inequality,

$$
\begin{aligned}
\Delta(\chi(t)) \leq C - \mathbb{E}\Bigg[& \sum_{j \in \mathcal{U}_R} (V\alpha g_R(\gamma_j(t)) - H_j(t)\gamma_j(t)) \\
& + \sum_{m \in \mathcal{U}_H} (V\beta g_H(\gamma_m(t)) - H_m(t)\gamma_m(t))|\chi(t) \Bigg] \\
- \mathbb{E}\Bigg[& \sum_{m \in \mathcal{U}_H} (H_m(t) - Q_m(t))R_m(t) \\
& + \sum_{j \in \mathcal{U}_R} (H_j(t) - Q_j(t))R_j(t)|\chi(t) \Bigg] \\
- \mathbb{E}\Bigg[& \sum_{m \in \mathcal{U}_H} Q_m(t)\mu_m(t)\tau + \sum_{j \in \mathcal{U}_R} Q_j(t)\mu_j(t)\tau \\
& + Z(t)(\mu_{sum}(t) - W\eta_{EE}^{req}p_{sum}(t))|\chi(t)\Bigg],
\end{aligned}
\tag{23}
$$

where C is a finite constant parameter that satisfies

$$
\begin{aligned}
C \geq \tfrac{1}{2}\mathbb{E}\Bigg[& (W\eta_{EE}^{req}p_{sum}(t))^2 + \mu_{sum}^2(t) + \sum_{j \in \mathcal{U}_R}(2R_j^2(t) + \\
& \mu_j^2(t)\tau^2 + \gamma_j^2) + \sum_{m \in \mathcal{U}_H}(2R_m^2(t) + \mu_m^2(t)\tau^2 + \gamma_m^2)|\chi(t)\Bigg].
\end{aligned}
\tag{24}
$$

Proof: Please refer to Appendix C. □

According to the theory of Lyapunov optimization, instead of minimizing the drift-minus-utility expression (22) directly, a good joint congestion control and resource optimization strategy can be obtained by minimizing the right hand side (R.H.S.) of (23) at each slot, which can be decoupled to a series of independent subproblems and can be solved concurrently with the real-time online observation of traffic queues and virtual queues at each slot.

C. Problem Decomposition

1) Auxiliary Variable Selection: The optimal auxiliary variables can be obtained by minimizing the first item of R.H.S. of (23) at each slot, i.e. $- \sum_{j \in \mathcal{U}_R} (V\alpha g_R(\gamma_j(t)) - H_j(t)\gamma_j(t)) - \sum_{m \in \mathcal{U}_H} (V\beta g_H(\gamma_m(t)) - H_m(t)\gamma_m(t))$. Since the auxiliary variables are independent among different UEs, the minimization can be decoupled to be computed for each UE separately as

$$
\begin{aligned}
\max_{\gamma_j(t)} \quad & V\alpha g_R(\gamma_j(t)) - H_j(t)\gamma_j(t) \\
\text{s.t.} \quad & \gamma_j(t) \leq A_j^{\max},
\end{aligned}
\tag{25}
$$

$$
\begin{aligned}
\max_{\gamma_m(t)} \quad & V\beta g_H(\gamma_m(t)) - H_m(t)\gamma_m(t) \\
\text{s.t.} \quad & \gamma_m(t) \leq A_m^{\max}.
\end{aligned}
\tag{26}
$$

Apparently, the problems above are both convex optimization problems. Therefore, the optimal auxiliary variables can

be derived by differentiating the objective function and make the result equal to zero. In the case of logarithmic utility function, we have $\gamma_j(t) = \min\left[\frac{V\alpha}{H_j(t)}, A_j^{\max}\right]$ and $\gamma_m(t) = \min\left[\frac{V\beta}{H_m(t)}, A_m^{\max}\right]$, where a larger $H_j(t)$ decreases $\gamma_j(t)$, which in turn avoids the further increase of $H_j(t)$.

2) Optimal Traffic Admission Control: The optimal traffic admission control can be obtained by minimizing the second item of R.H.S. of (22) at each slot, i.e. $\sum_{m \in \mathcal{U}_H} [H_m(t) - Q_m(t)]R_m(t) + \sum_{j \in \mathcal{U}_R} [H_j(t) - Q_j(t)]R_j(t)$. Similarly, it can be further decoupled to be computed for each UE separately as follows

$$
\begin{aligned}
\max_{R_m} \quad & (H_m(t) - Q_m(t))R_m(t) \\
\text{s.t.} \quad & R_m(t) \leq A_m(t),
\end{aligned}
\tag{27}
$$

$$
\begin{aligned}
\max_{R_j} \quad & (H_j(t) - Q_j(t))R_j(t) \\
\text{s.t.} \quad & R_j(t) \leq A_j(t),
\end{aligned}
\tag{28}
$$

which are linear problems with the following optimal solutions:

$$
R_m(t) = \begin{cases} A_m(t), & \text{if } H_m(t) - Q_m(t) > 0, \\ 0, & \text{else,} \end{cases}
\tag{29}
$$

$$
R_j(t) = \begin{cases} A_j(t), & \text{if } H_j(t) - Q_j(t) > 0, \\ 0, & \text{else.} \end{cases}
\tag{30}
$$

This is a simple threshold-based admission control strategy. When the traffic queue $Q_m(t)$ (or $Q_j(t)$) is smaller than a threshold $H_m(t)$ (or $H_j(t)$), then the newly traffic arrivals are admitted into the maintained traffic queues. Consequently, this not only reduces the value of $H_m(t)$ (or $H_j(t)$)so as to push $\gamma_m(t)$ (or $\gamma_j(t)$) to become closer to $R_m(t)$ (or $R_j(t)$), but also increases the throughput $R_m(t)$ (or $R_j(t)$) so as to improve the utility. On the other hand, when traffic queue $Q_m(t)$ or $(Q_j(t))$ is larger than a threshold $H_m(t)$ (or $H_j(t)$), then the traffic arrivals will be denied to ensure the stability of traffic queues.

3) Optimal User Association, RB and Power Allocation: The optimal user association, RB, and power allocation at slot t can be obtained by minimizing the remaining item of R.H.S. of (22), which is expressed as

$$
\begin{aligned}
\min_{\mathbf{s},\mathbf{p},\mathbf{a}} \quad & -\sum_{m \in \mathcal{U}_H} B_m(t)\mu_m(t) - \sum_{j \in \mathcal{U}_R} B_j(t)\mu_j(t) \\
& + Y_R(t)\sum_{i \in \mathcal{R}} p_i(t) + Y_H(t)p_H(t) \\
\text{s.t.} \quad & C1, C2, C3, C4, C8.
\end{aligned}
\tag{31}
$$

where $B_m(t) = Q_m(t)\tau + Z(t)$, $B_j(t) = Q_j(t)\tau + Z(t)$, $Y_R(t) = W\eta_{EE}^{req}\varphi_{eff}^R Z(t)$, $Y_H(t) = W\eta_{EE}^{req}\varphi_{eff}^H Z(t)$. However, since the transmission rate $\mu_m(t)$, $\mu_j(t)$ and the transmit power consumption $p_i(t)$ and $p_H(t)$ are functions of user association $s_m(t)$, RB allocation $a_{jk}(t)$, $a_{mk}(t)$ and $b_{ml}(t)$ and power allocation $p_{ijk}(t)$, $p_{imk}(t)$ and $p_{ml}(t)$, this subproblem is a mixed-integer nonconvex problem and is usually prohibitively difficult to solve. To address this challenge, the computationally efficient algorithm for this subproblem will be studied in the next section.

IV. Optimal User Association, RB and Power Allocation

In this section, we commit to an effective method to solve the subproblem of user association, RB and power allocation. The continuity relaxation of binary variables and the Lagrange dual decomposition method will be first utilized, upon which the optimal primal solution is then obtained. As this subproblem is optimized at each slot, the slot index t will be ignored for brevity.

A. Continuity Relaxation

The multiplicative binary variables are first removed as $x_{mk} = (1 - s_m)a_{mk}$ and $y_{ml} = (1 - s_m)b_{ml}$, where $x_{mk} \in [0, 1]$ and $y_{ml} \in [0, 1]$. The binary variables a_{jk}, x_{mk} and y_{ml} are then relaxed to take continuous values in [0,1]. Furthermore, to make the problem tractable, the auxiliary variables are introduced as $w_{ijk} = a_{jk}p_{ijk}$, $v_{imk} = x_{mk}p_{imk}$ and $u_{ml} = y_{ml}p_{ml}$. Let $\mathbf{x} = [a_{jk}, x_{mk}, y_{ml} : j \in \mathcal{U}_R, m \in \mathcal{U}_H, k \in \mathcal{K}_R, l \in \mathcal{K}_H]$ denote the vector of relaxed RB allocation variables. Let $\mathbf{w} = [w_{ijk}, v_{imk}, u_{ml} : i \in \mathcal{R}, j \in \mathcal{U}_R, m \in \mathcal{U}_H, k \in \mathcal{K}_R, l \in \mathcal{K}_H]$ denote the vector of introduced auxiliary variables. Thus the optimization problem (31) can be finally rewritten as

$$
\begin{aligned}
\min_{\mathbf{x},\mathbf{w}} &- \sum_{m \in \mathcal{U}_H} B_m \Big(\sum_{l \in \mathcal{K}_H} y_{ml}\log_2(1 + g_{ml}u_{ml}/y_{ml}) \\
&+ \sum_{k \in \mathcal{K}_R} x_{mk}\log_2(1 + \sum_{i \in \mathcal{R}} v_{imk}g_{imk}/x_{mk})\Big) \\
&- \sum_{j \in \mathcal{U}_R} B_j \sum_{k \in \mathcal{K}_R} a_{jk}\log_2(1 + \sum_{i \in \mathcal{R}} w_{ijk}g_{ijk}/a_{jk}) \\
&+ Y_R \sum_{i \in \mathcal{R}} \Big(\sum_{k \in \mathcal{K}_R}\sum_{m \in \mathcal{U}_H} v_{imk} + \sum_{k \in \mathcal{K}_R}\sum_{j \in \mathcal{U}_R} w_{ijk}\Big) \\
&+ Y_H \sum_{m \in \mathcal{U}_H}\sum_{l \in \mathcal{K}_H} u_{ml} \\
\text{s.t.} \quad &\sum_{j \in \mathcal{U}_R} a_{jk} + \sum_{m \in \mathcal{U}_H} x_{mk} \le 1, \forall k, \\
&\sum_{m \in \mathcal{U}_H} x_{ml} \le 1, \forall l, \\
&\sum_{k \in \mathcal{K}_R}\sum_{m \in \mathcal{U}_H} v_{imk} + \sum_{k \in \mathcal{K}_R}\sum_{j \in \mathcal{U}_R} w_{ijk} \le p_i^{\max}, \forall i, \\
&\sum_{m \in \mathcal{U}_H}\sum_{l \in \mathcal{K}_H} u_{ml} \le p_H^{\max}, \\
&a_{jk}, x_{mk}, y_{ml} \in [0, 1], \forall j, k, m, l.
\end{aligned}
\tag{32}
$$

Since the term $-x_{mk}\log_2(1 + \sum_{i \in \mathcal{R}} v_{imk}g_{imk}/x_{mk})$, $-y_{ml}\log_2(1 + g_{ml}u_{ml}/y_{ml})$ and $-a_{jk}\log_2(1 + \sum_{i \in \mathcal{R}} w_{ijk}g_{ijk}/a_{jk})$ are the perspective functions of convex functions $-\log_2(1 + \sum_{i \in \mathcal{R}} v_{imk}g_{imk})$, $-\log_2(1 + g_{ml}u_{ml})$ and $-\log_2(1 + \sum_{i \in \mathcal{R}} w_{ijk}g_{ijk})$, respectively, the objective of (32) is a convex function. Furthermore, the constraints of (32) are all linear with the continuity relaxation of binary variables. According to the Salter's condition, the zero Lagrange duality gap is guaranteed [26].

B. Dual Decomposition

The convex optimization problem can be solved by Lagrange dual decomposition. Specifically, the Lagrangian function of the primal objective function is given by

$$
\begin{aligned}
L(\boldsymbol{\lambda}) = \min_{\mathbf{x},\mathbf{w}} &- \sum_{m \in \mathcal{U}_H} B_m \Big(\sum_{l \in \mathcal{K}_H} y_{ml}\log_2(1 + u_{ml}g_{ml}/y_{ml}) \\
&+ \sum_{k \in \mathcal{K}_R} x_{mk}\log_2(1 + \sum_{i \in \mathcal{R}} v_{imk}g_{imk}/x_{mk})\Big) \\
&- \sum_{j \in \mathcal{U}_R} B_j \sum_{k \in \mathcal{K}_R} a_{jk}\log_2(1 + \sum_{i \in \mathcal{R}} w_{ijk}g_{ijk}/a_{jk}) \\
&+ \sum_{i \in \mathcal{R}} (Y_R + \theta_i)\Big(\sum_{k \in \mathcal{K}}\sum_{m \in \mathcal{U}_H} v_{imk} + \sum_{k \in \mathcal{K}_R}\sum_{j \in \mathcal{U}_R} w_{ijk}\Big) \\
&- \sum_{i \in \mathcal{R}} \theta_i p_i^{\max} + (Y_H + \theta_0) \sum_{m \in \mathcal{U}_H}\sum_{l \in \mathcal{K}_H} u_{ml} - \theta_0 p_H^{\max},
\end{aligned}
\tag{33}
$$

where $\boldsymbol{\theta} = [\theta_0, \theta_1, \theta_2, ..., \theta_N]$ is the vector of Lagrangian dual variables related to the HPN and RRH transmit power constraints. The Lagrangian dual function is given by

$$
\begin{aligned}
D(\boldsymbol{\theta}) = \min_{\mathbf{x},\mathbf{w}} &L(\boldsymbol{\theta}) \\
\text{s.t.} \quad &\sum_{m \in \mathcal{U}_H} y_{ml} \le 1, \forall l, \\
&\sum_{j \in \mathcal{U}_R} a_{jk} + \sum_{m \in \mathcal{U}_H} x_{mk} \le 1, \forall k, \\
&a_{jk}, x_{mk}, y_{ml} \in [0, 1], \forall j, k, m, l.
\end{aligned}
\tag{34}
$$

and the dual optimization problem is given by

$$
\begin{aligned}
\max_{\boldsymbol{\theta}} \quad &D(\boldsymbol{\theta}) \\
\text{s.t.} \quad &\boldsymbol{\theta} \succeq 0,
\end{aligned}
\tag{35}
$$

Based on the Karush-Kuhn-Tucker (KKT) conditions, the optimal power allocation can be obtained by differentiating the objective function of (33) with respect to v_{imk}, w_{ijk} and u_{ml}, which are given by

$$
v_{imk}^* = \left[\frac{B_m}{(Y_R + \theta_i)\ln 2} - \frac{1 + \sum_{i' \ne i} v_{i'mk}^* g_{i'mk}}{g_{imk}} \right]^+ x_{mk}, \tag{36}
$$

$$
w_{ijk}^* = \left[\frac{B_j}{(Y_R + \theta_i)\ln 2} - \frac{1 + \sum_{i' \ne i} w_{i'jk}^* g_{i'jk}}{g_{ijk}} \right]^+ a_{jk}, \tag{37}
$$

$$
u_{ml}^* = \left[\frac{B_m}{(Y_H + \theta_0)\ln 2} - \frac{1}{g_{ml}} \right]^+ y_{ml}, \tag{38}
$$

where $[x]^+ = \max\{x, 0\}$. The derived power allocations have the form of multi-level watering-filling and the water-filling levels are determined by the traffic queue states and the virtual queue state.

Substituting the optimal power allocations v_{imk}^*, w_{ijk}^* and u_{ml}^* into (33) and denoting

$$
\Phi_{mk} = \sum_{i \in \mathcal{R}} (Y_R + \theta_i)p_{imk} - B_m R_b \log_2(1 + \sum_{i \in \mathcal{R}} p_{imk}g_{imk}), \tag{39}
$$

$$
\Lambda_{jk} = \sum_{i \in \mathcal{R}} (Y_R + \theta_i)p_{ijk} - B_j R_b \log_2(1 + \sum_{i \in \mathcal{R}} p_{ijk}g_{ijk}), \tag{40}
$$

$$
\Gamma_{ml} = (Y_H + \theta_0)p_{ml} - B_m R_b \log(1 + g_{ml}p_{ml}), \tag{41}
$$

For notation simplicity, the dual function can be simplified as

$$\min_{\mathbf{x}} \sum_{m \in \mathcal{U}_H} \sum_{k \in \mathcal{K}_R} \Phi_{mk} x_{mk} + \sum_{m \in \mathcal{U}_H} \sum_{l \in \mathcal{K}_H} \Gamma_{ml} y_{ml} + \sum_{j \in \mathcal{U}_R} \sum_{k \in \mathcal{K}_R} \Lambda_{jk} a_{jk}$$
$$\text{s.t.} \sum_{m \in \mathcal{U}_H} y_{ml} \leq 1, \forall l,$$
$$\sum_{j \in \mathcal{U}_R} a_{jk} + \sum_{m \in \mathcal{U}_H} x_{mk} \leq 1, \forall k,$$
$$a_{jk}, x_{mk}, y_{ml} \in [0, 1], \forall j, k, m, l. \tag{42}$$

which is a linear programming (LP) problem. It can be proven that if the bounded linear programming problem has an optimal solution, then at least one of the optimal solutions is composed of the extreme points [27].

With the continuity relaxation, the optimal RB allocation and user association will be derived effectively according to the following scheme.

- For the RB k of RRH tier, the RB allocation to HUE m is decided by

$$x_{mk} = \begin{cases} 1, & \text{if } m = \arg\min\{\Phi_{mk} : m \in \mathcal{U}_H\} \\ & \&\Phi_{mk} < \min\{\Lambda_{jk} : j \in \mathcal{U}_R\} \\ & \&\Phi_{mk} < \min\{\Gamma_{ml} : l \in \mathcal{K}_H\}, \\ 0, & \text{else.} \end{cases} \tag{43}$$

If there is RB of RRH tier allocated to HUE m, then we have $s_m = 1$.

- The remaining RBs of RRH tier will be allocated to RUEs. Let $\mathcal{K}'_R$ denote the remaining RBs of RRH tier, then for RB $k \in \mathcal{K}'_R$, the a_{jk} is given by

$$a_{jk} = \begin{cases} 1, & \text{if } j = \arg\min\{\Lambda_{jk} : j \in \mathcal{U}_R\}\&\Lambda_{jk} < 0, \\ 0, & \text{else.} \end{cases} \tag{44}$$

- After the RB allocation of RRH tier is accomplished, the RBs of HPN tier will be allocated. Let $\mathcal{U}'_0$ denote the set of HUEs that are served by HPN. The RB allocation y_{ml} is given by

$$y_{ml} = \begin{cases} 1, & \text{if } m = \arg\min\{\Gamma_{ml} : m \in \mathcal{U}'_0\}, \\ 0, & \text{else.} \end{cases} \tag{45}$$

It is worth noting that, after the continuity relaxation, the binary x_{mk}, a_{jk} and y_{ml} can be still obtained at the extreme point of constraint set, i.e., 0 or 1.

To recover the optimal primal solution, the dual variables are then iteratively computed using the subgradient method [28],

$$\theta_0^{(n+1)} = \left[\theta_0^{(n)} + \xi_0^{(n+1)} \nabla_0^{(n+1)}\right]^+, \tag{46}$$

$$\theta_i^{(n+1)} = \left[\theta_i^{(n)} + \xi_i^{(n+1)} \nabla_i^{(n+1)}\right]^+, \tag{47}$$

where n is the iteration index, $\xi_0^{(n)}$ and $\xi_i^{(n)}$ is the step size at the n-th iteration to guarantee the convergence, $\nabla_0^{(n+1)}$ and $\nabla_i^{(n+1)}$ are the subgradient of the dual function, which are given by

$$\nabla_0^{(n+1)} = \left(\sum_{m \in \mathcal{U}_H} \sum_{l \in \mathcal{K}_H} u_{ml}^{(n)} - p_H^{\max}\right), \tag{48}$$

$$\nabla_i^{(n+1)} = \left(\sum_{j \in \mathcal{U}_R} \sum_{k \in \mathcal{K}_R} w_{ijk}^{(n)} + \sum_{j \in \mathcal{U}_R} \sum_{k \in \mathcal{K}_R} v_{imk}^{(n)} - p_i^{\max}\right). \tag{49}$$

Finally, the overall procedure of joint congestion control and resource optimization is summarized in the **Algorithm 1**.

Algorithm 1 The Joint Congestion Control and Resource Optimization Algorithm

---

1: For each slot, observe the traffic queues $Q_m(t)$, $Q_j(t)$ and the virtual queues $H_m(t)$, $H_j(t)$, $Z(t)$;
2: Calculate the optimal auxiliary variables $\gamma_m(t)$ and $\gamma_j(t)$ by solving (25) and (26);
3: Determine the optimal amount of admitted traffics $R_m(t)$ and $R_j(t)$ according to (29) and (30);
4: **repeat**
5:   Obtain the optimal power allocation p_{imk} and p_{ijk} of RRH tier by iteratively updating (36) and (37);
6:   Obtain the optimal power allocation p_{ml} of HPN according to (38);
7:   Obtain the optimal RB allocation a_{mk} and a_{jk} of RRH tier according to (43) and (44) and derive the optimal user association s_m;
8:   Obtain the optimal RB allocation b_{ml} of HPN tier according to (45);
9:   Update the Lagrangian dual variables $\boldsymbol{\theta}$ according to (46) and (47);
10: **until** certain stopping criteria is met;
11: Update the traffic queues $Q_m(t)$, $Q_j(t)$ and the virtual queues $H_m(t)$, $H_j(t)$ and $Z(t)$ according to (9), (10), (18), (19) and (20).

V. PERFORMANCE BOUNDS

In this section, the performance bounds of the proposed algorithm based on Lyapunov optimization will be mathematically analyzed.

A. Bounded Queues

Suppose ϕ_H and ϕ_R are the largest right-derivative of $g_H(.)$ and $g_R(.)$, respectively, then the proposed algorithm based on Lyapunov optimization ensures that the traffic queues are bounded, which is given by **Theorem** 3.

Theorem 3: For arbitrary traffic arrival rates (possibly exceeding the network capacity of H-CRAN) and certain EE requirement, an H-CRAN using the proposed algorithm with any $V \geq 0$ can guarantee the following bounds of traffic queues:

$$Q_j(t) \leq V\alpha\phi_R + 2A_j^{\max}, \tag{50}$$

$$Q_m(t) \leq V\beta\phi_H + 2A_m^{\max}. \tag{51}$$

Proof: Please refer to Appendix D. □

B. Utility Performance

The utility performance of proposed solution based on Lyapunov optimization is given by **Theorem 4**.

Theorem 4: For arbitrary arrival rates and certain EE requirement, an H-CRAN using the proposed algorithm with

any $V \geq 0$ *can provides the following utility performance under certain EE requirement:*

$$U(\bar{\mathbf{r}}) \geq U^* - C/V, \quad (52)$$

where U^* is the optimal infinite horizon utility over all algorithms that stabilize traffic queues and satisfy required EE performance constraint.

Proof: Please refer to Appendix E. □

To readily understand the obtained results indicated in **Theorem** 3 and **Theorem** 4, some important observations are further provided as follows.

- **Theorem** 4 shows that $U(\bar{\mathbf{r}}) \geq U^* - C/V$. Besides, $U(\bar{\mathbf{r}}) \leq U^*$. Therefore, we have $U^* - C/V \leq U(\bar{\mathbf{r}}) \leq U^*$, which indicates that $U(\bar{\mathbf{r}})$ can be arbitrarily close to U^* by setting a sufficiently large V to make C/V arbitrarily small and close to 0. This will be further verified in the following simulation section as shown in Fig. 2.
- **Theorem** 3 and **Theorem** 4 both show the delay-utility tradeoff of $[\mathcal{O}(V), 1 - \mathcal{O}(1/V)]$, which provides an important guideline to explicitly balance the delay-throughput performance on demand. This will also be further verified in the simulation section as shown in Fig. 2 and Fig. 3.

Remark 1: The traffic models are not specified throughout this paper, as they do not affect the problem formulation and the corresponding analysis. Moreover, although the packet traffic arrivals with i.i.d. and constant arrival rates are considered in this paper, the proposal and the corresponding theoretical analysis results still hold for other arrivals that are independent from slot to slot, but their arrival rates are time-varying and ergodic (possibly non-i.i.d.). The reason is that the joint congestion control and resource optimization policy is made only based on the size of the queues without requiring the knowledge of traffic arrivals. Therefore, the proposal is robust to the traffic arrival distribution model.

VI. SIMULATIONS

In this section, simulations will be carried out to evaluate the performances of proposed Joint-Congestion-Control-and-Resource-Optimization (JCCRO) scheme in an H-CRAN.

A. Parameters Setting

The considered H-CRAN consists of 1 HPN, 4 RRHs, 12 HUEs and 10 RUEs. The HPN is located in the center of the cell area, while the RRHs, HUEs and RUEs are uniformly distributed. There are 8 RBs and 12 RBs in the RB sets $\mathcal{K}_H$ and $\mathcal{K}_R$, respectively. The bandwidth of each RB is $W_0 = 15$ kHz, so the system bandwidth is $W = 300$ kHz. The slot duration is 0.01 second. The path loss model of RRH and HPN is given by $31.5 + 40.0 \log 10(d)$ and $31.5 + 35.0 \log 10(d)$, respectively, where d denotes the distance between transmitter and receiver in meters. The fast-fading coefficients are all generated as i.i.d. Rayleigh random variables with unit variances. The noise power is -102 dBm. For the HPN, the drain efficiency, the maximum transmit power consumption and the static power consumption are given by $\varphi_{\text{eff}}^H = 1$,
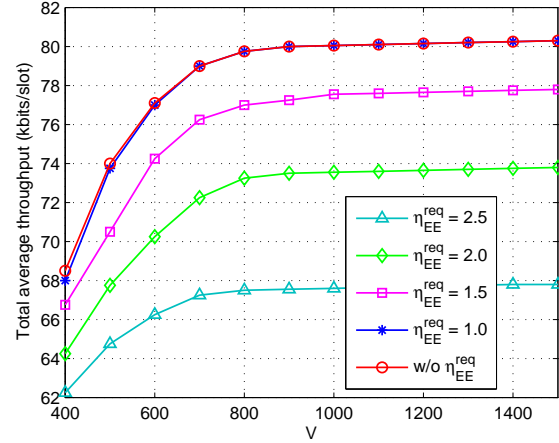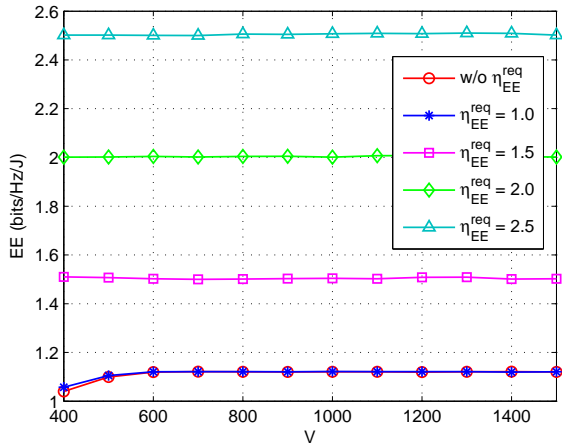

Fig. 2. Total average throughput versus control parameter V

$p_H^{\max} = 10$ W, $p_c^H = 2$ W, respectively. For the RRHs, the drain efficiency, the total transmit power consumption and the static power consumption are given by $\varphi_{\text{eff}}^R = 1$, $p_i^{\max} = 3$ W, $p_c^R = 1$ W, respectively. For simplicity of comparison, the utility function of total average throughput is adopted, i.e. $U(\bar{\mathbf{r}}) = \alpha \sum_{j \in \mathcal{U}_R} \bar{r}_j + \beta \sum_{m \in \mathcal{U}_H} \bar{r}_m$, where the positive utility prices for RUEs and HUEs are $\alpha = 1$ and $\beta = 1$, respectively. It is worth noting that in this special case, the first subproblem to derive optimal auxiliary variables is not required. The traffic arrivals of HUEs and RUEs follow Poisson distribution, and the mean traffic arrival rate for RUE λ_j and HUE λ_m is given by $\lambda_j = \lambda$ and $\lambda_m = 0.5\lambda$, respectively. Each point of the following curves is averaged over 5000 slots.

B. The Delay-Throughput Tradeoff with Guaranteed EE

Fig. 2 and Fig. 3 illustrate the performances of throughput, delay with guaranteed EE versus different control parameter V when the mean traffic arrival rate is $\lambda = 6$ kbits/slot. As can be seen, the achieved utility of total average throughput increases to optimum at the speed of $\mathcal{O}(1/V)$ as V increases, which is due to the fact that a larger V implies that the control solution emphasizes more on throughput utility. However, the utility improvement starts to diminish with excessive increase of V, which can adversely aggravate the congestion as the average delay increases linearly with V. All these verify the observations indicated by **Theorem** 3 and **Theorem** 4. Furthermore, Fig. 4 plots the achieved EE verses different control parameter V, which shows that the achieved EE is always larger than or equal to $\eta_{\text{EE}}^{\text{req}}$.
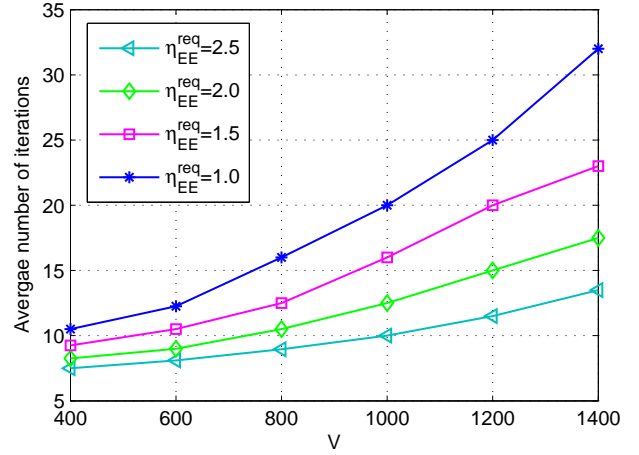
It can be further observed from Fig. 2 - Fig. 4 that there exists a ceratin EE threshold $\eta_{\text{EE}}^{\text{thr}}$ of the network when making a tradeoff between delay and throughput. In our simulations, the EE threshold is $\eta_{\text{EE}}^{\text{thr}} = 1.12$, which is actually the EE archived by the case without EE requirement. Specifically, when the required EE is below $\eta_{\text{EE}}^{\text{thr}}$, the actually achieved EE and delay-throughput tradeoff is almost the same as the situation without EE requirement. Once the required EE is above the threshold $\eta_{\text{EE}}^{\text{thr}}$, the total average throughput sharply
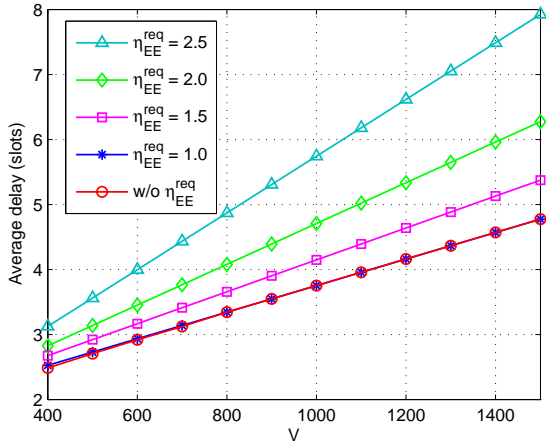
Fig. 3.   Average delay versus control parameter V

Fig. 5.   Average number of convergence iterations versus control parameter V

Fig. 4.   Achieved EE versus control parameter V

decreases (see Fig. 2), and the average delay also increases (see Fig. 3). This is because, to guarantee the required EE, the network has to decrease the transmit power, which further result in the decrease of transmit rate, followed by the decrease of achieved throughput and the increase of average delay. All the above observations indicate that the network can guarantee the EE performance when maximizing the throughput. At this point, the control parameter V provides a controllable method to flexibly balance throughput-delay performance tradeoff with guaranteed EE. To let the H-CRAN work in a preferred state, what we only need to do is to select an appropriate control parameters V.

C. The Convergence of The Proposed Solution

Fig. 5 shows the average number of convergence iterations for the proposal. It can be generally observed that the proposal under different EE requirements can converge fairly fast. Besides, the convergence speed is influenced by some key parameters. On the one hand, a larger V means a larger average sum rate and then a slower convergence. On the other hand, as clarified in Fig. 2, a larger EE requirement η_{EE}^{req} makes a smaller average sum rate, which means a faster convergence.

### D. The Performance Comparison under Different Traffic Arrival Rate

To validate the efficacy of the proposed JCCRO scheme, we compare its performances with the Maximum-Sum-Rate (MSR) scheme, which is modeled as

$$\max \sum_{j \in \mathcal{U}_R} \mu_j(t) + \sum_{m \in \mathcal{U}_H} \mu_m(t) \\ \text{s.t. } C1 - C5, C8.$$ (53)

For the JCCRO scheme, we set the control parameter as $V = 1000$. From Fig. 6, it can be observed that the total average transmit rate of the proposed JCCRO scheme with different EE requirement are the same and not less than the total traffic arrival rate at first, then go to the maximum values as the mean traffic arrival rate increases. From Fig. 7, it can be observed that the average delay of the proposed JCCRO scheme always increases with increasing mean arrival rate, that is because more traffic arrivals means larger transmit rate, which cannot be large enough due to the EE constraint. Again, the results of Fig. 6 and Fig. 7 confirm that the setting of EE requirement have a great effect on system performance.

As for the compared MSR scheme, on the one hand, the total average transmit rate keeps unchanged as the traffic arrival rate varies (see Fig. 6). The reason is that the MSR scheme does not consider stochastic traffic arrivals and delivers data under the full buffer assumption. On the other hand, the average delay of MSR scheme is almost the same as that of JCCRO scheme at first, but it begins to sharply increase to infinity as time elapse when the arrival rate is large than a certain value(see. Fig. 7). This is because both schemes are able to timely transmit all the arrived data when the arrival rate is small, while the traffic admission control component of JCCRO starts to work to make the queues stable as the arrival rates increase.

In Fig. 8, we further compare the total avergae power consumption of the JCCRO scheme and the MSR scheme. We can see that the power consumption of MSR scheme keeps unchanged as traffic arrival rate varies and is much more than that of JCCRO scheme in the relatively light traffic states. This is because that the MSR scheme delivers data
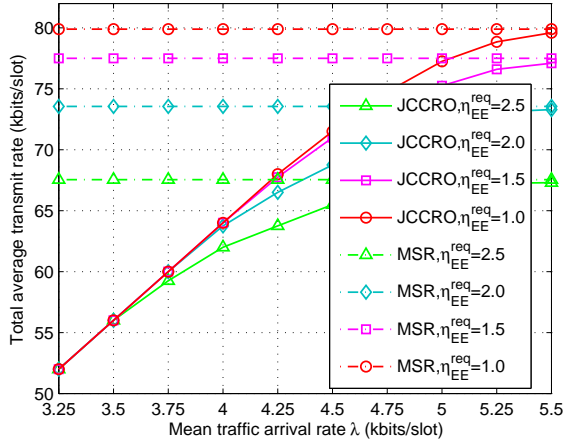
Fig. 6.   Total average transmit rate versus mean traffic arrival rate λ
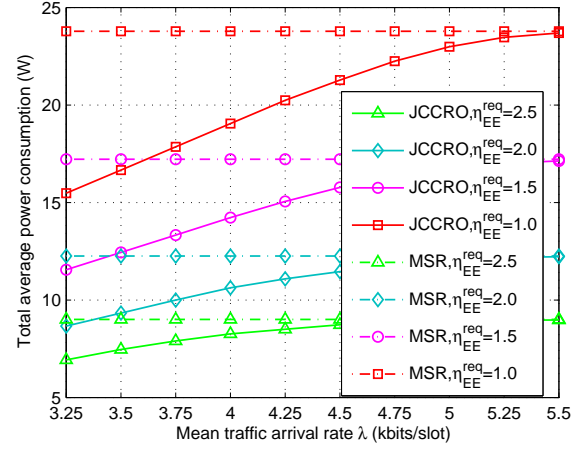
Fig. 8.   Total average power consumption versus mean traffic arrival rate λ
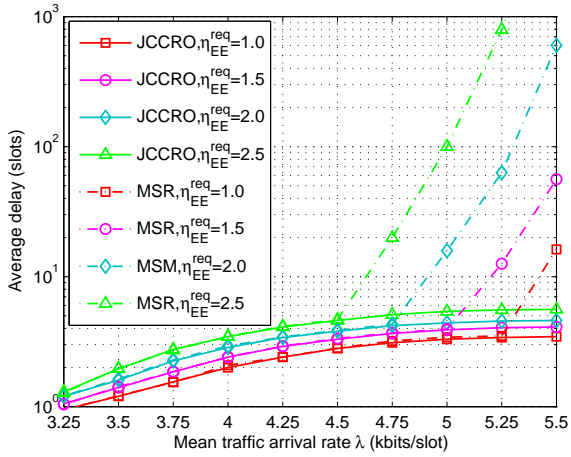
Fig. 7.   Average delay versus mean traffic arrival rate λ

under the full buffer assumption and fails to adapt to the traffic arrivals, which thus leads to a waste of energy despite achieving the same EE performance. All the observations from Fig. 6 - Fig. 8 validate the advantages of joint congestion control and resource optimization: 1) in the relative light traffic states, more energy can be saved with the adaptive resource optimization, and 2) in the relative heavy traffic states, the traffic queues can be stabilized with the traffic admission control.

VII. CONCLUSION

This work has focused on the stochastic optimization of EE-guaranteed joint congestion control and resource optimization in a downlink slotted H-CRAN. Based on the Lyapunov optimization technique, this stochastic optimization problem has been transformed and decomposed into three subproblems which are solved at each slot. The continuality relaxation of binary variables and Lagrange dual decomposition method have been exploited to solve the third subproblem efficiently. An EE-guaranteed $[\mathcal{O}(1/V), \mathcal{O}(V)]$ throughput-delay tradeoff has been finally achieved by the proposed scheme, which has

been verified by both the mathematical analysis and numerical simulations. The simulation results have shown the significant impact of EE requirement on the achieved throughput-delay tradeoff and have validated the significant advantages of joint congestion control and resource optimization. For the future work, it would be interesting to extend our proposed model to provide deterministic delay guarantee for real-time traffic applications in realistic networks, e.g., mobile video and voice.

APPENDIX A
PROOF OF THEOREM 1

Let U_1^* and U_2^* be the optimal utility of problems (16) and (17), respectively. For ease of notation, let Ω_1^* and Ω_2^* be the optimal solutions that achieve U_1^* and U_2^*, respectively. Since $U(.)$ is a non-decreasing concave function, by Jensen's inequality, we have

$$U(\bar{\gamma}) \geq \bar{U}(\gamma) = U_2^*. \qquad (54)$$

Since the solution Ω_2^* satisfies the constraint C10, then we have

$$U(\bar{r}) \geq U(\bar{\gamma}). \qquad (55)$$

Furthermore, since Ω_2^* is feasible for the transformed problem (17), it also satisfies the constraints of the original problem (16). Therefore, we can have

$$U_1^* \geq U(\bar{r}) \geq U_2^*. \qquad (56)$$

Now we prove that $U_2^* \geq U_1^*$. Since Ω_1^* is an optimal solution to the original problem, it satisfies the constraints C1-C8, which are also the constraints of the transformed problem. By choosing $\gamma_m = \bar{r}_m^*$ and $\gamma_j = \bar{r}_j^*$ for all slot t together with the policy Ω_1^*, we then have a feasible policy for the transformed problem (17), that is

$$U_2^* \geq \bar{U}(\gamma) = U(\bar{r}) = U_1^*. \qquad (57)$$

Therefore, we have $U_1^* = U_2^*$ and can further conclude the **Theorem** 1.

APPENDIX B
PROOF OF THEOREM 2

The constraint C5 is proved firstly, and C10 can be proved similarly. When the virtual queue $H_j(t)$ is stable, then we have $\lim_{T\to\infty} \frac{\mathbb{E}[H_j(T)]}{T} = 0$ with the probability 1. It is clear that $H_j(t+1) \geq H_j(t) - R_j(t) + \gamma_j(t)$. Summing this inequality over time slots $t \in \{0, 1, ..., T-1\}$ and dividing the result by T yields

$$\frac{H_j(T) - H_j(0)}{T} + \frac{1}{T}\sum_{t=0}^{T-1} R_j(t) \geq \frac{1}{T}\sum_{t=0}^{T-1}\gamma_j(t). \quad (58)$$

By taking T asymptotically closed to infinity, we finally have C5.

It is similarly concluded that we can have the inequality $W\eta_{\text{EE}}^{\text{req}}\bar{p}_{\text{sum}} \leq \bar{\mu}_{\text{sum}}$, i.e. $\eta_{\text{EE}} \geq \eta_{\text{EE}}^{\text{req}}$, only when the virtual queue $Z(t)$ is stable.

APPENDIX C
PROOF OF LEMMA 1

By leveraging the fact that $(\max[a-b,0]+c)^2 \leq a^2+b^2+c^2-2a(b-c), \forall a,b,c \geq 0$ and squaring Eq. (9), Eq. (10), Eq. (18), Eq. (19) and Eq. (20), we have

$$Q_m^2(t+1) - Q_m^2(t) \leq R_m^2(t) + \mu_m^2(t)\tau^2 - 2Q_m(t)(\mu_m(t)\tau - R_m(t)), \quad (59)$$

$$Q_j^2(t+1) - Q_j^2(t) \leq R_j^2(t) + \mu_j^2(t)\tau^2 - 2Q_j(t)(\mu_j(t)\tau - R_j(t)), \quad (60)$$

$$H_m^2(t+1) - H_m^2(t) \leq \gamma_m^2(t) + R_m^2(t) - 2H_m(t)(R_m(t) - \gamma_m(t)), \quad (61)$$

$$H_j^2(t+1) - H_j^2(t) \leq \gamma_j^2(t) + R_j^2(t) - 2H_j(t)(R_j(t) - \gamma_j(t)), \quad (62)$$

$$Z^2(t+1) - Z^2(t) \leq (W\eta_{\text{EE}}^{\text{req}}p_{\text{sum}}(t))^2 + \mu_{\text{sum}}^2(t) - 2Z(t)(\mu_{\text{sum}}(t) - W\eta_{\text{EE}}^{\text{req}}p_{\text{sum}}(t)). \quad (63)$$

According to the definition of Lyapunov drift, we then have the following expression by summing up the above inequalities and taking expectation over both sides,

$$\mathbb{E}[L(\chi(t+1) - L(\chi(t))] \leq$$
$$\frac{1}{2}\sum_{j\in\mathcal{U}_R}\mathbb{E}[2R_j^2(t) + \mu_j^2(t)\tau^2 + \gamma_j^2] + \frac{1}{2}\sum_{m\in\mathcal{U}_H}\mathbb{E}[2R_m^2(t) + \mu_m^2(t)\tau + \gamma_m^2]$$
$$+ \mathbb{E}[W^2(\eta_{\text{EE}}^{\text{req}})^2 p_{\text{sum}}^2(t) + \mu_{\text{sum}}^2(t)] - \sum_{j\in\mathcal{U}_R}\mathbb{E}[Q_j(t)(\mu_j(t)\tau - R_j(t))]$$
$$-\sum_{m\in\mathcal{U}_H}\mathbb{E}[Q_m(t)(\mu_m(t) - R_m(t))] - \sum_{j\in\mathcal{U}_R}\mathbb{E}[H_j(t)(R_j(t) - \gamma_j(t))]$$
$$-\sum_{m\in\mathcal{U}_H}\mathbb{E}[H_m(t)(R_m(t) - \gamma_m(t))] - \mathbb{E}[Z(t)(\mu_{\text{sum}}(t) - W\eta_{\text{EE}}^{\text{req}}p_{\text{sum}}(t))], \quad (64)$$

Finally, the upper bound of drift-minus-utility expression can be obtained as Eq. (22) by subtracting the expression $V\mathbb{E}\{U(\gamma)\}$ from the both sides of Eq. (64).

APPENDIX D
PROOF OF THEOREM 3

The bounds of traffic queues for RUEs are proved firstly, and that for MUEs can be proved similarly. Suppose that the following inequality holds at slot t,

$$H_j(t) \leq V\alpha\phi_R + A_j^{\text{max}}, \quad (65)$$

If $H_j(t) \leq V\alpha\phi_R$, then it is easy to get $H_j(t) \leq V\alpha\phi_R + A_j^{\text{max}}$ according to the admission constraint $R_j(t) \leq A_j^{\text{max}}$. Else if $H_j(t) \geq V\alpha\phi_R$, since the utility function $g_R(.)$ is a non-decreasing concave function and ϕ_R is the largest right-derivative of $g_R(.)$, the following inequality can be easily established,

$$V\alpha g_R(\gamma_j(t)) - H_j(t)\gamma_j(t) \leq V\alpha g_R(0) + (V\alpha\phi_R - H_j(t))\gamma_j(t) \leq V\alpha g_R(0). \quad (66)$$

which follows that when $H_j(t) \geq V\alpha\phi_R$, the auxiliary variables decision in (25) forces γ_j to be 0. Therefore, inequality (65) also holds at slot $t+1$,

$$H_j(t+1) \leq H_j(t) \leq V\alpha\phi_R + A_j^{\text{max}}. \quad (67)$$

With above bound of virtual queue, the bound of traffic queue is proved next. If $Q_j(t) \leq H_j(t)$, according to the admission control policy in (30), we have

$$Q_j(t+1) = Q_j(t) + R_j(t) \leq Q_j(t) + A_j^{\text{max}} \leq H_j(t) + A_j^{\text{max}} = V\alpha\phi_R + 2A_j^{\text{max}}. \quad (68)$$

APPENDIX E
PROOF OF THEOREM 4

To prove the bound of utility performance, the following lemma is required.

Lemma 2: For arbitrary arrival rates, there exists a randomized stationary control policy π for H-CRAN that chooses feasible control decisions independent of current traffic queues and virtual queues, which yields the following steady state values:

$$\gamma_m^\pi(t) = r_m^*, \gamma_j^\pi(t) = r_j^*, \quad (69)$$

$$\mathbb{E}[R_m^\pi(t)] = r_m^*, \mathbb{E}[R_j^\pi(t)] = r_j^*, \quad (70)$$

$$\mathbb{E}[\mu_m^\pi(t)\tau] \geq \mathbb{E}[R_m^\pi(t)], \mathbb{E}[\mu_j^\pi(t)\tau] \geq \mathbb{E}[R_j^\pi(t)], \quad (71)$$

$$\mathbb{E}[\mu_{\text{sum}}^\pi(t)] \geq W\eta_{\text{EE}}^{\text{req}}\mathbb{E}[p_{\text{sum}}^\pi(t)]. \quad (72)$$

As the similar proof of **Lemma** 2 can be found in [29], the details are omitted to avoid redundancy. Since the proposed solution is obtained by choosing control variables that can minimize the R.H.S. of Eq. (22) among all feasible decisions (including the randomized control decision π in **Lemma** 2) at each slot, then we have

$$\Delta(\chi(t)) \leq C - \mathbb{E}\left[\sum_{j\in\mathcal{U}_R}(V\alpha g_R(\gamma_j^\pi(t)) - H_j(t)\gamma_j^\pi(t))\right.$$
$$\left. + \sum_{m\in\mathcal{U}_H}(V\beta g_H(\gamma_m^\pi(t)) - H_m(t)\gamma_m^\pi(t))|\chi(t)\right]$$
$$- \mathbb{E}\left[\sum_{m\in\mathcal{U}_H}(H_m(t) - Q_m(t))R_m^\pi(t)\right.$$
$$\left. + \sum_{j\in\mathcal{U}_R}(H_j(t) - Q_j(t)]R_j^\pi(t))\chi(t)\right]$$
$$- \mathbb{E}\left[\sum_{m\in\mathcal{U}_H}Q_m(t)\mu_m^\pi(t)\tau + \sum_{j\in\mathcal{U}_R}Q_j(t)\mu_j^\pi(t)\tau\right.$$
$$\left. + Z(t)(\mu_{\text{sum}}^\pi(t) - W\eta_{\text{EE}}^{\text{req}}p_{\text{sum}}^\pi(t))|\chi(t)\right], \quad (73)$$

Since the randomized stationary policy is independent of $\chi(t)$, we have

$$\Delta(\chi(t)) \leq C - \sum_{j\in\mathcal{U}_R}[\mathbb{E}[V\alpha g_R(\gamma_j^\pi(t))] - H_j(t)\mathbb{E}[\gamma_j^\pi(t)]]$$
$$+\sum_{m\in\mathcal{U}_H}[\mathbb{E}[V\beta g_H(\gamma_m^\pi(t))]-H_m(t)\mathbb{E}[\gamma_m^\pi(t)]]-\sum_{m\in\mathcal{U}_H}(H_m(t)$$
$$-Q_m(t))\mathbb{E}[R_m^\pi(t)] - \sum_{j\in\mathcal{U}_R}(H_j(t)-Q_j(t))\mathbb{E}[R_j^\pi(t)]$$
$$-\sum_{m\in\mathcal{U}_H}Q_m(t)\mathbb{E}[\mu_m^\pi(t)\tau] - \sum_{j\in\mathcal{U}_R}Q_j(t)\mathbb{E}[\mu_j^\pi(t)\tau]$$
$$-Z(t)(\mathbb{E}[\mu_{sum}^\pi(t)] - W\eta_{EE}^{req}\mathbb{E}[p_{sum}^\pi(t)]), \tag{74}$$

By plugging (70)-(72) into the R.H.S. of (74), we have

$$\mathbb{E}[L(\chi(t+1)) - L(\chi(t))] - V\mathbb{E}[U(\gamma(t))] \leq C - VU^*. \tag{75}$$

Then by summing the above over slot $t \in \{0,1,...T-1\}$ and dividing the result by T, we have

$$\frac{\mathbb{E}[L(\chi(t+1))] - \mathbb{E}[L(\chi(0))]}{T} - \frac{1}{T}\sum_{t=0}^{T-1}\mathbb{E}[U(\gamma(t))] \leq C - VU^*. \tag{76}$$

Considering the fact that $L(\chi(t+1)) \geq 0$ and $L(\chi(0)) = 0$, we then have

$$\lim_{T\to\infty}\frac{1}{T}\sum_{t=0}^{T-1}\mathbb{E}[U(\gamma(t))] \geq U^* - C/V. \tag{77}$$

Furthermore, since the utility function is a non-decreasing concave function, according to Jensen's inequality, we finally have

$$U(\bar{\mathbf{r}}) \geq U(\bar{\gamma}) \geq \frac{1}{T}\sum_{t=0}^{T-1}\mathbb{E}[U(\gamma(t))] \geq U^* - C/V. \tag{78}$$

REFERENCES

[1] C. I, C. Rowell, S. Han, Z. Xu, Gang Li, and Z. Pan, "Toward green and soft: a 5G perspective," *IEEE Commun. Mag.*, vol. 52, no. 2, pp. 66-73, Feb. 2014.
[2] C. Wang, F. Haider, X. Gao, X. You, Y. Yang, D. Yuan, H. Aggoune, H. Haas, S. Fletcher, and E. Hepsaydir, "Cellular architecture and key technologies for 5G wireless communication networks," *IEEE Commun. Mag.*, vol. 52, no. 2, pp. 122-130, Feb. 2014.
[3] P. Rost, C. J. Bernardos, A. D. Domenico, M. D. Girolamo, M. Lalam, A. Maeder, D. Sabella, and D. Wübben, "Cloud technologies for flexible 5G radio access networks, *IEEE Commun. Mag.*, vol. 52, no. 5, pp. 68-76, May 2014.
[4] K. Chen, *et. al.*,"C-RAN: the road towards green RAN," whitepaper, ver. 2.5, China Mobile Research Institute, Oct. 2011.
[5] M. Peng, Y. Li, J. Jiang, J. Li, and C. Wang, "Heterogeneous cloud radio access networks: a new perspective for enhancing spectral and energy efficiencies," *IEEE Wireless Commun.*, vol. 21, no. 6, pp. 126-135, Dec. 2014.
[6] M. Peng, Y. Li, Z. Zhao, and C. Wang, "System architecture and key technologies for 5G heterogeneous cloud radio access networks," *IEEE Network*, vol. 29, no. 2, pp. 6-14, Mar. 2015.
[7] D. Feng, C. Jiang, G. Lim, L. J. Cimini Jr., G. Feng, and G. Y. Li, "A survey of energy-efficient wireless communications," *IEEE Commun. Surveys & Tutorials*, vol. 15, no. 1, pp. 167-178, Feb. 2013.
[8] X. Hong, Y. Jie, C. Wang; J. Shi, and X. Ge, "Energy-spectral efficiency trade-off in virtual MIMO cellular systems," *IEEE J. Sel. Areas Commun.*, vol. 31, no. 10, pp. 2128-2140, Oct. 2013.
[9] O. Onireti, F. Heliot, and M. A. Imran, "On the energy efficiency-spectral efficiency trade-off of distributed MIMO systems," *IEEE Trans. Commun.*, vol. 61, no. 9, pp. 3741-3753, Sep. 2013.
[10] C. He, B. Sheng, P. Zhu, X. You. and G. Y. Li, "Energy- and spectral-efficiency tradeoff for distributed antenna systems with proportional fairness," *IEEE J. Sel. Areas Commun.*, vol. 31, no. 5, pp. 2128-2140, May 2013.
[11] K. Cheung, S. Yang, and L. Hanzo, "Spectral and energy spectral efficiency optimization of joint transmit and receive beamforming based multi-relay MIMO-OFDMA cellular networks," *IEEE Trans. Wireless Commun.*, vol. 13, no. 11, pp. 6147-6165, Nov. 2014.
[12] W. Jing, Z. Lu, X. Wen, Z. Hu, and S. Yang, "Flexible resource allocation for joint optimization of energy and spectral efficiency in OFDMA multi-cell networks," *IEEE Commun. Lett.*, vol. 19, no. 3, pp. 451-454, Mar. 2015.
[13] C. Xiong, G. Y. Li, S. Zhang, Y. Chen, and S. Xu, "Energy- and spectral-efficiency tradeoff in downlink OFDMA networks," *IEEE Trans. Wireless Commun.*, vol. 10, no. 11, pp. 3874-3886, Nov. 2011.
[14] S. Huang, H. Chen, J. Cai, and F. Zhao, "Energy efficiency and spectral-efficiency tradeoff in amplify-and-forward relay networks," *IEEE Trans. Veh. Tech.*, vol. 62, no. 9, pp. 4366-4378, Nov. 2013.
[15] I. Ku, C. Wang, and J. Thompson, "Spectral-energy efficiency tradeoff in relay-aided cellular networks," *IEEE Trans. Wireless Commun.*, vol. 12, no. 10, pp. 4970-4982, Oct. 2013.
[16] Z. Zhou, M. Dong, K. Ota, J. Wu, and T. Sato, "Energy efficiency and spectral efficiency tradeoff in Device-to-Device (D2D) communications," *IEEE Wireless Commun. Lett.*, vol. 3, no. 5, pp. 485-488, Oct. 2014.
[17] V. K. N. Lau and Y. Cui, "Delay-optimal power and subcarrier allocation for OFDMA systems via stochastic approximation," *IEEE Trans. Wireless Commun.*, vol. 9, no. 1, pp. 227-233, Jan. 2010.
[18] Y. Cui and V. K. N. Lau, "Distributive stochastic learning for delay-optimal OFDMA power and subband allocation," *IEEE Trans. Signal Process.*, vol. 58, no. 9, pp. 4848-4858, Sep. 2010.
[19] H. K. Chung and V. K. N. Lau, "Tradeoff analysis of delay-power-CSIT quality of dynamic backpressure algorithm for energy efficient OFDM system," *IEEE Trans. Signal Process.*, vol. 60, no. 8, pp. 4254-4263, Aug. 2012.
[20] Y. Li, M. Sheng, Y. Zhang, X. Wang, and J. Wen, "Energy-efficient antenna selection and power allocation in downlink distributed antenna systems: a stochastic optimization approach," in *Proc. IEEE ICC'14*, Sydney, Australia, Jun. 2014, pp. 4963-4968.
[21] V. K. N. Lau, F, Zhang, and Y. Cui, "Low complexity delay-constrained beamforming for multi-user MIMO systems with imperfect CSIT," *IEEE Trans. Signal Process.*, vol. 61, no. 16, pp. 4090-4099, Aug. 2013.
[22] M. J. Neely, "Delay-based network utility maximization," in *IEEE Proc. IEEE INFOCOM*, San Diego, USA, Mar. 2010, pp. 1145-1149.
[23] H. Ju, B. Liang, J. Li and X. Yang, "Dynamic joint resource optimization for LTE-Advanced relay networks," *IEEE Trans. Wireless Commun.*, vol. 12, no. 11, pp. 5668-5678, Nov. 2013.
[24] Y. Li, M. Sheng, Y. Shi, X. Ma, W, Jiao, "Energy efficiency and delay tradeoff for time-varying and interference-free wireless networks," *IEEE Trans. Wireless Commun.*, vol. 13, no. 11, pp. 5921-5931, Nov. 2014.
[25] Y. Cui, V. K. N. Lau, R. Wang, H. Huang, and S. Zhang, "A survey on delay-aware resource control for wireless systems - large deviation theory, stochastic Lyapunov drift, and distributed stochastic learning," *IEEE Trans. Inf. Theory*, vol. 58, no. 3, pp. 1677-1701, Mar. 2012.
[26] S. Boyd and L. Vandenberghe, *Convex Optimization*. Cambridge University Press, 2004.
[27] G. B. Dantzig and M. N. Thapa, *Linear Programming II-Theory and Extensions*. New York: Springer Series in Operations Research, 2003.
[28] S. Boyd (2008), *Subgradient methods*(lecture notes). Available: http://www.stanford.edu/class/ee364b/lectures/subgrad methodslides.pdf.
[29] M. J. Neely, *Stochastic network optimization with application to communication and queueing systems*, Morgan & Claypool Publishers, 2010.